

# FREQUENCY LOCKED LOOPS OF THE THIRD AND HIGHER ORDER

DJURDJE PERIŠIĆ

**Key words:** Frequency locked loops, Time non-recursive processing, Phase locked loop, Digital circuits.

This work describes a new model of frequency locked loop (FLL) with three outputs, which is based on the time measurement and non-recursive processing of the input periods only. FLL is a linear discrete system of the third order. All mathematical analyzes were performed using the Z transform approach. The general form of difference equation, describing FLL of any order, is developed and compared with the corresponding difference equation of digital filters. Analysis of FLL was performed in the time and frequency domain. It was shown that the Matlab tools, dedicated to FIR (Finite Impulse Response) digital filters, can be used for the analysis of FLL in the frequency domain. FLL is very fast. Depending on the choice of the system parameters, FLL can be used for the tracking and predicting applications, digital filtering of pulse periods, as well as in the applications of FLL which require short transient time. Computer simulation of FLL in the time domain is made to enable precise insight into the FLL properties.

## 1. INTRODUCTION

In this article, just like in ref. [1], we use term "non-recursive" in the expression time non-recursive processing (TNP), which originates from the FIR (finite impulse response) digital filter theory. The term "non-recursive" indicates that the calculation of the output periods is based solely on the measured periods of the input signal. Unlike [1], time recursive processing (TRP) phase locked loop (PLL) and frequency locked loop (FLL), described in refs. [2–9], are also defined in form of the linear difference equations, but these systems calculate the next output period using the input periods, the previous output periods, and the time differences between them. It was emphasized through [1–9], that TRP PLL, TRP FLL and TNP FLL appeared as completely new theory and design to PLL and FLL, which provide new PLL and FLL properties and enlarged the field of their applications in comparison to the classical PLLs and FLLs. TRP PLLs and FLLs are described in the applications of phase shifting, time shifting, phase control, frequency synthesizers, tracking, predicting, noise rejections, frequency multipliers, frequency measurement, and the others, what was highlighted in [1–9]. The articles and books in [10–22] are used as theoretical base, for electronics implementations and for the development necessities.

## 2. THE GENERAL FORM OF DIFFERENCE EQUATION OF TNP FLL OF HIGHER ORDER

Besides the description and analyzes of one model of TNP FLL, this article discovered that TNP FLL is, in many ways, very similar to FIR digital filters. The understanding of the similarities and differences between TNP FLL and FIR digital filters will enable the usage of the digital FIR filter Matlab tools, for the analyzes and design of TNP FLLs. Let us remember that non-recursive processing of FIR digital filter is described by eq. (1), where the output of a digital filter  $y(k)$  is the sum of products of  $(M+1)$  filter coefficients  $b_0, b_1, b_2, \dots, b_M$  and the corresponding samples of the input signal  $x(k-i)$ . Note that the variable "k", represents the discrete time  $t_k$  when an amplitude of the input signal is sampled, measured, and taken in calculation. According to eq. (1), there are  $(M+1)$  calculations of the outputs with  $(M+1)$  filter coefficients.

$$y(k) = \sum_{i=0}^M b_i \cdot x(k-i). \quad (1)$$

Before we try to define a general difference equation of TNP FLL of any order, analogue to eq. (1), let us consider Fig. 1, which represents a general case of an input signal  $S_{in}$  and an output signal  $S_{op}$  of TNP FLL. In comparison to the classical PLL and FLL, the input and output frequencies are changed by the input and output periods in Fig. 1, and the phase differences are changed by the time differences. The periods  $TI_k$  and  $TO_k$ , as well as the time difference  $\tau_k$ , occur at discrete times  $t_k, t_{k+1}, t_{k+2}, \dots, t_{k+M}, t_{k+M+1}$ , which are defined by the falling edges of the pulses of  $S_{op}$  in Fig. 1.

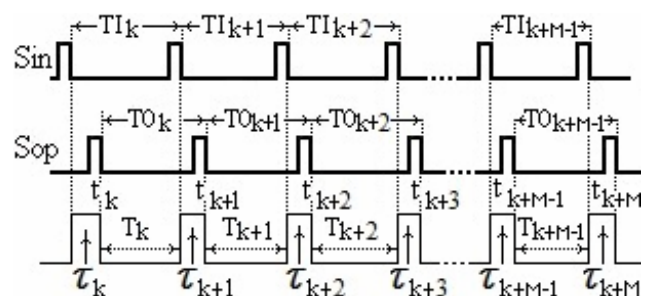


Fig. 1 – The time relations between the input and output variables of TNP FLL.

The first important difference between the processing described by eq. (1) and the processing of TNP FLL is the fact that instead of the amplitudes, TNP FLL uses the input periods in the processing. Secondly, unlike the amplitudes in eq. (1), which are defined at the proper discrete time  $t_k$ , the input and output periods  $TI_k$  and  $TO_k$  as well as time differences  $\tau_k$ , are distributed in time in Fig 1, so that every input period overlaps with the output period of the same order. Due to this distribution in time and overlapping, it is not possible to calculate, for instance, the output period  $TO_{k+1}$  as a function of  $TI_{k+1}$ , because the calculation of  $TO_{k+1}$  must be finished up to discrete time  $t_{k+1}$ , i.e., before the input period  $TI_{k+1}$  is expired (Fig. 1). At discrete time  $t_{k+1}$  the realization of  $TO_{k+1}$  should start. In other word, in the real time applications, any output period can be calculated only using the previous input periods of the lower order. Taking this fact in account, the general difference equation which describes TNP FLL, intended for

the real time applications, are presented in eq. (2). In comparison to eq. (1),  $y(k)$  is changed with  $TO(k)$ ,  $x(k-i)$  is changed with  $TI(k-i)$  and finally, " $i$ " starts from  $i = 1$ , instead of  $i = 0$ , in accordance with the previous conclusion that in the calculations of the outputs of TNP FLL, the inputs of the same order can not be used. The extended form of eq. (2) is shown in eq. (3). It comes out from eq. (3), that there are  $M$  system parameters of TNP FLL. These are  $b_1, b_2, \dots, b_M$ .  $M$  input periods are needed to complete the calculation of  $TO(k)$  with all system parameters. To facilitate the analyzes, let us choose that the beginning of  $M$  calculations starts at discrete time  $t = t_k$ , just like in Fig. 1. To do this let us change  $k = k+M$  into eq. (3), which will transform into eq. 4. Because of simplicity, all discrete times in brackets are changed with the corresponding index

$$TO(k) = \sum_{i=1}^M b_i \cdot TI(k-i), \quad (2)$$

$$TO(k) = b_1 \cdot TI(k-1) + b_2 \cdot TI(k-2) + \dots + b_M \cdot TI(k-M), \quad (3)$$

$$TO_{k+M} = b_1 TI_{k+M-1} + b_2 TI_{k+M-2} + \dots + b_M TI_k, \quad (4)$$

$$TO_{k+M} = \sum_{i=1}^M b_i \cdot TI_{k+M-i}, \quad (5)$$

marks in eq. 4. At last, eq. 4 can be written in shorted form, shown in eq. (5). Extended eq. (4) or its shorted form, shown in eq. (5), are adapted to correspond to Fig. 1. This adapting is useful for better understanding and monitoring of the future time analyzes and usage of the initial conditions.

Note that the filter coefficients of FIR digital filter, in eq. (1), are  $b_0, b_1, b_2, \dots, b_M$ , and the system parameters of TRP FLL, according to eq. (4), are  $b_1, b_2, \dots, b_M$ . Therefore, in usage of the tools of FIR filter for the frequency analyzes of TNP FLL, it is necessary to place  $b_0 = 0$  in Matlab commands. However, in those applications where FLL does not necessarily need to work in real time, it is possible to modify eq. (5) to correspond exactly to eq. (1), *i.e.*, in this case the variable  $i$  would take values from  $i = 0$  to  $M$ , instead of  $i = 1$  to  $M$ , as it is in eq. (5). In such applications, the output pulse signal would be generated with the corresponding delay.

## 2. ANALYSES OF TNP FLL OF THE THIRD ORDER IN TIME DOMAIN

Choosing  $M$  in eq. (4), it is possible to define a difference equation for a NTP FLL of any order. If we choose  $M = 3$  eq. (4) will be transformed into eq. (6), which represents the difference equation for TNP FLL of the third order. Since the precise recognition of the transient state of TNP FLL is very important for its applications, one additional difference equation, describing the time difference, is presented in eq. (7). It comes out as natural relation between the variables in Fig. 1. At last, the third variable  $T_k$ , presented in eq. (8), also represents the natural relation between the variables. So, the behavior of TNP FLL is precisely described by three outputs  $TO_k, \tau_k$  and  $T_k$ .

To determine the transfer functions of TNP FLL, the Z transform of eqs. (6), (7) and (8) are presented in eqs. (9),

(10) and (11), respectively, where  $TO_0, TO_1, TO_2$  and  $TI_0$  in eq. (9) and  $\tau_0$  in eq. (10) represent the initial conditions of variables  $TO_k, TI_k$  and  $\tau_k$ . Since the process start at  $t = t_k$ , all values of variables, before  $t = t_k$ , are equal zeros. Therefore, according to eq. (6),  $TO_1 = b_1 \cdot TI_0$  and  $TO_2 = b_1 \cdot TI_1 + b_2 \cdot TI_0$ . Entering  $TO_1$  and  $TO_2$  into eq. (9),  $TO(z)$  is calculated and presented in eq. (12).

$$TO_{k+3} = b_1 \cdot TI_{k+2} + b_2 \cdot TI_{k+1} + b_3 \cdot TI_k, \quad (6)$$

$$\tau_{k+1} = \tau_k + TO_k - TI_k, \quad (7)$$

$$T_k = TI_k - \tau_k, \quad (8)$$

$$z^3 TO(z) - z TO_2 - z^2 TO_1 - z^3 TO_0 = z^2 b_1 TI(z) - z b_1 TI_1 - z^2 b_1 TI_0 + z b_2 TI(z) - z b_2 TI_0 + b_3 TI(z), \quad (9)$$

$$z\tau(z) - z\tau_0 = \tau(z) + TO(z) - TI(z), \quad (10)$$

$$T(z) = TI(z) - \tau(z), \quad (11)$$

$$TO(z) = TI(z) \frac{z^2 b_1 + z b_2 + b_3}{z^3} + TO_0. \quad (12)$$

It is now of interest to investigate under which conditions this TNP FLL possesses the properties of a FLL. To do that, let us suppose that the step input is  $TI(k) = TI = \text{constant}$ . Substituting the Z transform of  $TI(k)$ , *i.e.*,  $TI(z) = TI \cdot z/(z-1)$  into eq. (12) and using the final value theorem, it is possible to find the final value of the output period  $TO$ , which TNP FLL reaches in the stable state. We can calculate  $TO_\infty = \lim TO(k)$  for  $k \rightarrow \infty$ , using  $TO(z)$ . This is shown in eq. (13).

It comes out from eq. (13), that  $TO_\infty = TI$  if eq. (14) is satisfied. TNP FLL possesses the properties either of a FLL or of a PLL, if eq. (14) is satisfied. To make decision, it is necessary to determine the behaviour of time difference  $\tau$ . Entering  $TO(z)$  from eq. (12), into eq. (10) and taking in account eq. (14),  $\tau(z)$  is calculated and presented in eq. (15). Substituting now  $TI(z) = TI \cdot z/(z-1)$  into eq. (15) and using the final value theorem, it is possible to find the final value of the time difference  $\tau_\infty = \lim \tau(k)$  for  $k \rightarrow \infty$ , using  $\tau(z)$ . This is shown in eq. (16). Equation (16) also confirms that TNP FLL possesses the properties of a FLL, since  $\tau_\infty$  depends on the initial conditions. It comes out that the system does not possess the properties of a PLL. At last, let us substitute eq. (15) and  $TI(z) = TI \cdot z/(z-1)$  into eq. (8) and find out  $T(z)$ , shown in eq. (17).

$$TO_\infty = \lim_{z \rightarrow 1} [(z-1)TO(z)] = TI(b_1 + b_2 + b_3), \quad (13)$$

$$b_1 + b_2 + b_3 = 1, \quad (14)$$

$$\tau(z) = TI(z) \frac{-z^2 + z(b_1 - 1) - b_3}{z^3} + \frac{TO_0 + z\tau_0}{z-1}, \quad (15)$$

$$\tau_\infty = \lim_{z \rightarrow 1} [(z-1)\tau(z)] = TI(b_1 - b_3 - 2) + TO_0 + \tau_0, \quad (16)$$

$$T(z) = TI(z) \frac{z^3 + z^2 - z(b_1 - 1) + b_3}{z^3} - \frac{TO_0 + z\tau_0}{z-1}. \quad (17)$$

There are three transfer functions, which describe TNP FLL. These are  $H_{TO}(z)$ ,  $H(z)$  and  $H_T(z)$  shown in eqs. (18), (19) and (20). They originate from eqs. (12), (15) and (17).

$$H_{TO}(z) = \frac{TO(z)}{TI(z)} = \frac{z^2 b_1 + z b_2 + b_3}{z^3}, \quad (18)$$

$$H_z(z) = \frac{\tau(z)}{TI(z)} = \frac{-z^2 + z(b_1 - 1) - b_3}{z^3}, \quad (19)$$

$$H_T(z) = \frac{T(z)}{TI(z)} = \frac{z^3 + z^2 - z(b_1 - 1) + b_3}{z^3}. \quad (20)$$

The simulations using Matlab tools can confirm all reached results. The simulations are to enable better insight into the procedures and physical meaning of the variables described. All discrete values in simulations were merged to form continuous curves. Note that all variables in the following diagrams were presented in time units. The time unit can be,  $\mu\text{sec}$ ,  $\text{msec}$  or any other, but assuming the same time units for all time variables  $TI$ ,  $TO$ ,  $\tau$  and  $T$ , it was more suitable to use just "time unit" or abbreviated "t.u." in the text. It was more convenient to omit the indication "t.u." in diagrams.

The simulations of  $TO(k)$  and  $\tau(k)$  for the step input  $TI_k = 10$  t.u., are shown in Fig. 2a. All values for three cases of different parameters  $b_1$ ,  $b_2$  and  $b_3$ , initial conditions and final values are shown in Fig. 2a. The system parameters satisfy eq. (14) in all cases and therefore, the output periods reached the input periods. According to eq. (16), using the values of parameters and the initial conditions presented in Fig. 2a, it can be calculated that  $\tau_{1\infty} = TI(b_1 - b_3 - 2) + TO_0 + \tau_0 = 10 \cdot (0.6 - 0.1 - 2) + 11 + 0 = -4$  t.u.

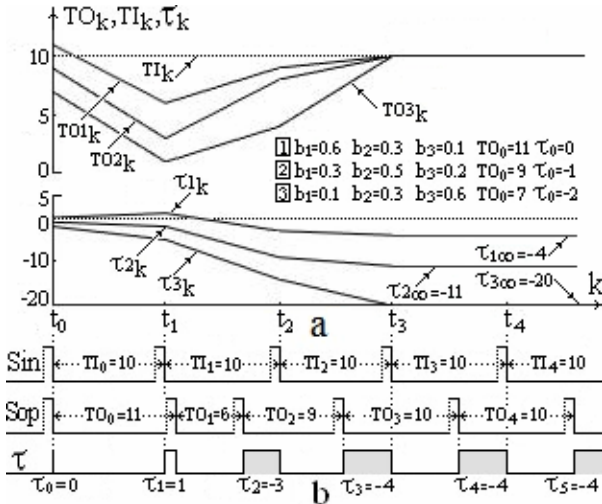


Fig. 2 – a) transition states of FLL for the step input; b) time relation between  $Sin$ ,  $Sop$  and  $\tau_k$  for the simulated case No. 1.

This result agrees with the simulated  $\tau_{1\infty}$ , shown in Fig. 2a. In the same way, it can be calculated that  $\tau_{2\infty} = -11$  t.u., and  $\tau_{3\infty} = -20$  t.u. The calculated values  $\tau_{2\infty}$ , and  $\tau_{3\infty}$  also agree with the simulated  $\tau_{2\infty}$ , and  $\tau_{3\infty}$  presented in Fig. 2a. These simulation results prove the correctness of the mathematical description and step analyses. The real time relation between  $Sin$ ,  $Sop$  and  $\tau_k$ , for the simulated case No. 1, is shown in Fig. 2b. For the stable TNP FLL, period  $TO_{\infty} = TI = 10$  t.u. and  $\tau_{\infty} = -4$  t.u. Note that FLL is very fast. It takes only three

steps to reach the stable state. FLL takes only one step to reach the stable state, looking from the discrete time when all parameters  $b_1$ ,  $b_2$  and  $b_3$  are taken in calculation, no matter of the values of parameters, providing that they satisfy eq. (14). To estimate if TNP FLL can track the ramp input, it is necessary to determine well-known velocity error  $K_V$ . If the input period is a ramp function  $TI(k) = TI_V(k) = p \cdot k$ , where  $p$  is a time constant,  $TI(z) = TI_V(z) = Z(p \cdot k) = pz/(z-1)^2$ . Generally, velocity error  $K_V = \lim_{k \rightarrow \infty} [TO_V(k) - TI_V(k)]$  for  $k \rightarrow \infty$ . One more suitable expression for velocity error is  $K_V = \lim_{k \rightarrow \infty} TI_V(k)[H_{TO}(k) - 1]$  for  $k \rightarrow \infty$ . Using the condition  $b_1 + b_2 + b_3 = 1$  and the final value theorem,  $K_V$  is calculated using eq. (18), and shown in eq. (21). According to eq. (21), TNP FLL can track the velocity input with the constant error. However, if  $2b_1 + b_2 = 3$ ,  $K_V = 0$ , i.e., TNP FLL can track a velocity input without any error.

$$K_V = \lim_{z \rightarrow 1} \left\{ (z-1) TI_V(z) [H_{TO}(z) - 1] \right\} = p \cdot (2b_1 + b_2 - 3). \quad (21)$$

Let us now determine the behaviour of  $\tau_v(k)$  for the velocity input, if  $k \rightarrow \infty$ , taking in account the previous condition  $2b_1 + b_2 = 3$ . Using the final value theorem,  $\tau_{v\infty} = \lim_{k \rightarrow \infty} \tau_v(k)$  is calculated using  $\tau_v(z)$  and shown in eq. (22). The expression  $\tau_v(z)$  in eq. (22) is found out by the substitution of  $TI(z) = TI_V(z) = pz/(z-1)^2$  into eq. (15). According to eq. (22),  $\tau_{v\infty}$  is the time constant. Besides the initial conditions  $TO_0$  and  $\tau_0$ ,  $\tau_{v\infty}$  depends on the time constant  $p$ , which is the slope of the ramp input function, as well as on the system parameters. But if  $b_1 = 3$ ,  $\tau_{v\infty}$  depends only on the initial conditions  $TO_0$  and  $\tau_0$ . The simulations of  $TO(k)$ ,  $K_V$  and  $\tau(k)$  for the velocity input  $TI_k = (10+4 \cdot k)$  t.u., are shown in Fig. 3. All values for two cases of different parameters  $b_1$ ,  $b_2$  and  $b_3$ , initial conditions

$$\tau_{v\infty} = \lim_{z \rightarrow 1} \left[ (z-1) \tau_v(z) \right]_{z \rightarrow 1} = p(b_1 - 3) + TO_0 + \tau_0, \quad (22)$$

and final values are shown in Fig. 3. The case No. 1 match both conditions  $b_1 + b_2 + b_3 = 1$  and  $2b_1 + b_2 + 3 = 0$ . According to eq. (21),  $K_{V1} = p(2b_1 + b_2 - 3) = 4 \cdot (2 \cdot 1 + 1 - 3) = 0$  t.u. This calculated result agrees with  $K_{V1}$  in Fig. 3. The case No. 2 matches  $b_1 + b_2 + b_3 = 1$ , but it does not match  $2b_1 + b_2 + 3 = 0$ . According to eq. (21),  $K_{V2} = p(2b_1 + b_2 - 3) = 4 \cdot [2 \cdot 1.2 + (-0.8) - 3] = -5.6$  t.u. This result also agrees with  $K_{V2}$  simulated in Fig. 3. At last, according to eq. (22),  $\tau_{1\infty} = p(b_1 - 3) + TO_0 + \tau_0 = 4(1 - 3) + 5 + 2 = -1$  t.u.

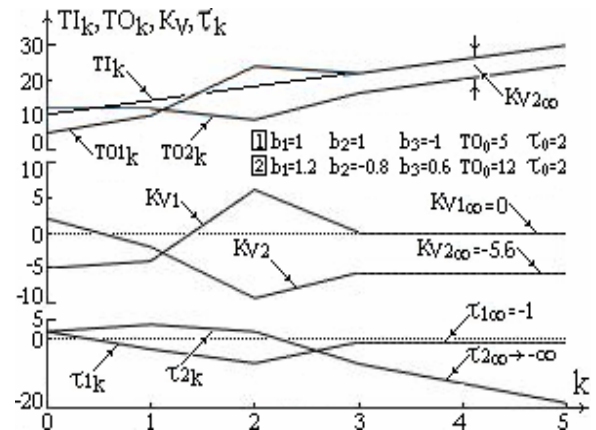


Fig. 3 – Simulation of the input and output variables in the tracking of the ramp function  $TI_k = 10 + 4 \cdot k$  t.u.

This result agrees with  $\tau_{1\infty}$  simulated in Fig. 3. Simulated  $\tau_{2\infty} \rightarrow -\infty$  in Fig. 3, what agrees with the fact that  $K_{V2}$  is not equal to zero, *i.e.*,  $K_{V2} < 0$ . Note that, even for the ramp input, demonstrated in Fig. 3, all the outputs of TNP FLL take only three steps to reach the stable state, just like for the step inputs in Fig. 2. All simulated values  $K_{V1}$ ,  $K_{V2}$ , and  $\tau_{1\infty}$  agree with the calculated ones by eqs. (21) and (22), proving so the correctness of the previous analyzes. The identity of the analytical and simulation results, in every step, proves the correctness of the entire theoretical approach, as well as the validity of all results obtained.

Let us now estimate if TNP FLL can track an accelerated input  $TI(k) = TI_A(k) = p \cdot k^2$ , where  $p$  is the time constant. The accelerated error  $K_A$  is defined as  $K_A = \lim_{k \rightarrow \infty} [TO_A(k) - TI_A(k)]$  for  $k \rightarrow \infty$ . One more suitable expression is  $K_A = \lim_{k \rightarrow \infty} TI_A(k)[H_{TO}(k) - 1]$  for  $k \rightarrow \infty$ . Z transform of  $TI_A(k)$  is  $TI_A(z) = p \cdot z(z+1)/(z-1)^3$ . Using the conditions  $b_1+b_2+b_3 = 1$ ,  $2b_1+b_2 = 3$ , then eq. (18) and the final value theorem,  $K_A$  is calculated and shown in eq. (23). According to eq. (23), TNP FLL can track the accelerated input

$$K_A = \lim_{z \rightarrow 1} \left\{ (z-1) TI_A(z) [H_{TO}(z) - 1] \right\} = 2p \cdot (b_1 - 3), \quad (23)$$

with the constant error. However, if  $b_1 = 3$ ,  $K_A = 0$ , *i.e.*, TNP FLL can track an accelerated input without an error. If  $b_1 = 3$ ,  $b_2$  and  $b_3$  can be calculated from the previous conditions as  $b_2 = -3$  and  $b_3 = 1$ . The simulations of  $TO(k)$  and  $K_A(k)$  for the accelerated input  $TI_k = (10+4 \cdot k^2)$  t.u., are shown in Fig. 4. All values for three cases of different parameters  $b_1$ ,  $b_2$  and  $b_3$ , initial conditions and final values are shown in Fig. 4. The case No. 1 satisfies all of three conditions  $b_1+b_2+b_3 = 1$ ,  $2b_1+b_2 = 3$  and  $b_1 = 3$ . The case No. 2 satisfies two conditions  $b_1+b_2+b_3 = 1$  and  $2b_1+b_2 = 3$  and the case No. 3 satisfies only the condition for the system stability  $b_1+b_2+b_3 = 1$ .

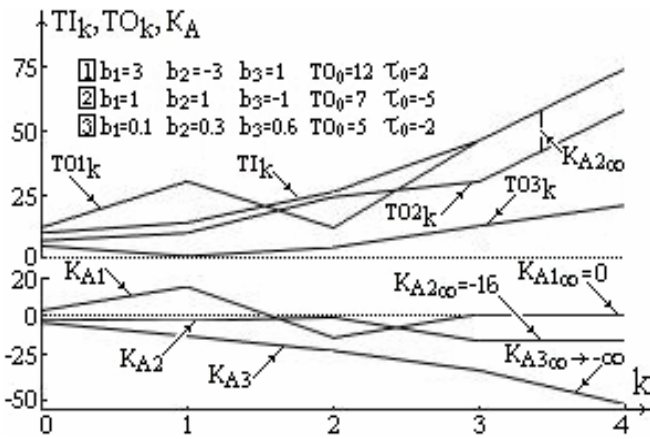


Fig. 4 – Simulation of the input and output variables in the tracking of the accelerated function  $TI_k = 10 + 4 \cdot k^2$  t.u.

We can see in Fig. 4, that in case No. 1, TNP FLL tracks the accelerated input without an error. In case No. 2, TNP FLL tracks the input with the constant error  $K_{A2}$ . For the case No. 3, TNP FLL is not able to track the input, since  $K_{A3} \rightarrow -\infty$ . According to eq. (23),  $K_{A1} = 2p \cdot (b_1 - 3) = 2 \cdot 4 \cdot (3 - 3) = 0$  t.u. and  $K_{A2} = 2p \cdot (b_1 - 3) = 2 \cdot 4 \cdot (1 - 3) = -16$  t.u. These calculated results agree with the simulated  $K_{A1}$  and  $K_{A2}$  in Fig. 4, proving the correctness and validity of all results obtained.

Note that, even for the accelerated input, shown in Fig. 4, all the outputs of TNP FLL take only three steps to reach the stable state, just like for the step and velocity inputs.

### 3. ANALYZES OF TNP FLL OF THE THIRD ORDER IN FREQUENCY DOMAIN

The structural similarity between eq. (1) for FIR digital filters and eq. (5) for TNP FLLs gives us right to use Matlab tools, designed for FIR filters, in the development and frequency analyzes of TNP FLLs. One example of this usage is in detail carried out in ref. [1], for TNP FLL of the second order. Let us remind that all FIR filter tools are developed for the processing of the amplitudes of the input signals and that TNP FLL processes the periods of the input signals. However, if the system transfer function of TNP FLL is exactly determined and its parameters properly entered Matlab tools, then, regardless of the type of input and output variables, Matlab tools are equally usable. However, it is necessary to understand the physical meaning of the variables and properly interpret the results obtained. One important additional difference between FIR digital filters and TNP FLL is the fact that TNP FLL is described by three transfer functions  $H_{TO}(z)$ ,  $H_\tau(z)$  and  $H_T(z)$ . The usage of additional transfer functions  $H_\tau(z)$  and  $H_T(z)$  comes out from the need for the knowledge about the time relation between the input and output signal of TNP FLL, taking in account the initial conditions. The additional benefit in usage of three outputs comes out from the fact that different transfer functions possess different filter characteristics.

Let us first present the magnitude and the frequency responses for three transfer functions  $H_{TO}(z)$ ,  $H_\tau(z)$  and  $H_T(z)$ , shown in eqs. (18) to (20). For this purpose, Matlab command “freqz”, in the interval  $(0, \pi)$  rad, is used. The vectors  $\mathbf{a}$  and  $\mathbf{b}$  which are to be entered in the command “freqz”, corresponding to  $H_{TO}(z)$ ,  $H_\tau(z)$  and  $H_T(z)$ , are  $\mathbf{a}_{TO} = [1 \ 0 \ 0 \ 0]$ ,  $\mathbf{b}_{TO} = [0 \ \mathbf{b}_1 \ \mathbf{b}_2 \ \mathbf{b}_3]$ ,  $\mathbf{a}_\tau = \mathbf{a}_{TO}$ ,  $\mathbf{b}_\tau = [0 \ -1 \ (\mathbf{b}_1 - 1) \ -\mathbf{b}_3]$ ,  $\mathbf{a}_T = \mathbf{a}_{TO}$  and  $\mathbf{b}_T = [1 \ 1 \ -(\mathbf{b}_1 - 1) \ \mathbf{b}_3]$ . The chosen parameters for TNP FLL are  $b_1 = -1$ ,  $b_2 = 3$  and  $b_3 = -1$ . The sampling frequency  $f_s = 1200$  Hz corresponds to the whole interval  $(0, \pi)$  rad, so that  $f_s/2 = 600$  Hz, covers the interval  $(0, \pi)$  rad.

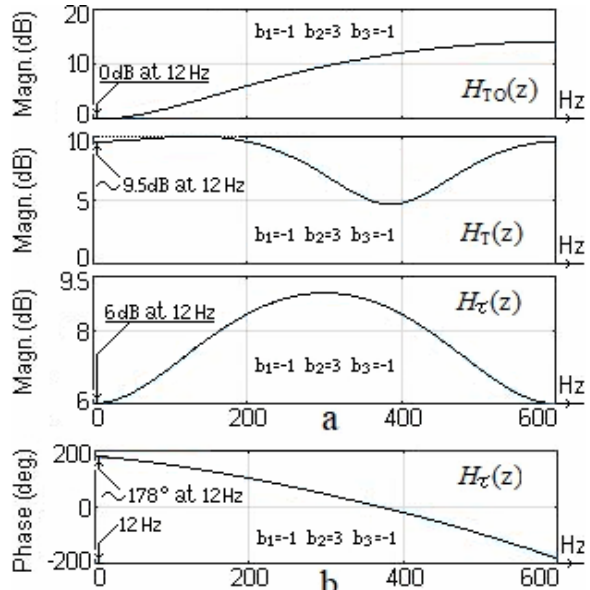


Fig. 5 – a) Magnitudes of the frequency responses of  $H_{TO}(z)$ ,  $H_T(z)$  and  $H_\tau(z)$ ; b) phase of the frequency response of  $H_\tau(z)$ .



The frequency responses are shown in Figs. 5a, and 5b. Number of time steps is chosen to be  $k = 1\,200 = f_s$ . The angular sampling step is  $\omega_s = 2\pi/1\,200$  rad. To establish a visible connection between time and frequency domains of TNP FLL, time presentations of TI and  $\tau$  is shown in Fig. 6 for  $TO_0 = 0$ ,  $TI_0 = 10$  and  $\tau_0 = 0$ . The input signal is the input period TI, as  $TI(k) = 10 + S_{12}$ , where  $S_{12} = A_{TI} \sin[(2\pi/f_s) \cdot f_m \cdot k]$ . The input period TI(k) can be considered as the constant period of 10 t.u., which is modulated by the samples of sinusoidal signal  $S_{12}$ . It was chosen  $A_{TI} = 8$  t.u.,  $f_m = 12$  Hz and  $k = 300$  in Fig. 6. Every of 12 periods of  $S_{12}$  will be sampled by 1 200 samples/12 periods = 100 samples/period. This provides sufficiently good resolution of TI and  $\tau$  in Fig. 6.

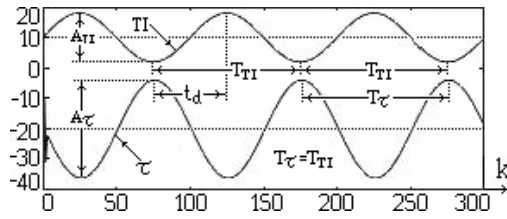


Fig. 6 – Presentation of TI and  $\tau$  in time domain for  $b_1 = -1$ ,  $b_2 = 3$ ,  $b_3 = -1$ ,  $TO_0 = 0$  and  $\tau_0 = 0$ .

To be compared with the frequency presentation of TI and  $\tau$ , only 300 first steps of  $k$  are presented in Fig. 6, covering three of twelve periods of TI. At last, Matlab commands "fft" and "stem" are used for the generation of the spectrums of TI, TO, T and  $\tau$  in Fig. 7. These spectrums present the absolute values of amplitudes, covering the whole interval  $(0, \pi)$  rad. They appear as positive values in the symmetric second half  $(\pi, 2\pi)$  rad.

We can see in Fig. 5a, that for the same system parameters, TNP FLL offers three different magnitudes of frequency responses, corresponding to three transfer functions. Transfer function  $H_{TO}(z)$  functions as a high-pass filter,  $H_T(z)$  functions as a band-pass filter and  $H_\tau(z)$  behaves as an inverted band-pass filter. In other word, only one TNP FLL, covers the functioning of three different digital filters.

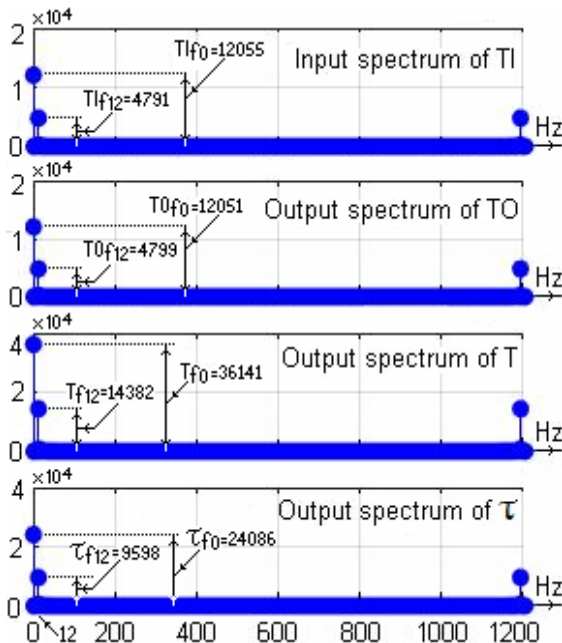


Fig. 7 – Spectra of TI, TO, T and  $\tau$  in frequency domain for  $b_1 = -1$ ,

For the same system parameters, they offer the different filter characteristics. Note that in the frequency domain, shown in Fig. 7, every one of three digital filter outputs contain both, the component at 0 Hz, corresponding to period  $TI = 10$  t.u. and the component at 12 Hz, corresponding to signal  $S_{12}$ . Due to this property, TNP FLL offers wide abilities for digital filtering of the pulse periods. The filter edges in Fig. 5a are not too sharp. Using TRP FLL of a higher order and choosing the corresponding system parameters, it would be possible to generate sharper band edges, just like with the digital FIR filters.

Let us now make a closed loop of time-frequency checks to verify that the frequency responses in Fig. 5, spectrums shown in Fig. 7 and the time presentation in Fig. 6, correspond each to other. Comparisons will be made independently for the constant of 10 t.u. and sinusoidal signal. The constant of 10 t.u. of  $TI(k)$ , appears as very strong amplitude with the frequency of 0 Hz in all spectrums of TI, TO, T and  $\tau$ . Their values are found in simulation listing and shown in Fig. 7. The amplitude of TI spectrum at frequency of 0 Hz is  $TI_{f0} = 12\,055$  t.u. and the amplitude of TO spectrum at frequency of 0 Hz is  $TO_{f0} = 12\,051$  t.u. in Fig. 7. The attenuation of zero component of TI, at the output TO is  $20 \log(TO_{f0}/TI_{f0}) = 20 \log(12\,051/12\,055) \sim 0$  dB. The magnitude of  $H_{TO}(z)$  at 0 Hz, in Fig. 5a, shows the same result. In the same way, the amplifications of zero component of TI at the output spectrums of T and  $\tau$  can be calculated respectively as  $20 \log(T_{f0}/TI_{f0}) = 20 \log(36\,141/12\,055) = 9.53$  dB and  $20 \log(\tau_{f0}/TI_{f0}) = 20 \log(24\,086/12\,055) = 6.03$  dB. Very close to these results, show the magnitudes of  $H_T(z)$  and  $H_\tau(z)$  at 0 Hz, in Fig. 5a. The sinusoidal signal  $S_{12}$  at 12 Hz also appears in all spectrums in Fig. 7. Their values, taken from simulation listing, are shown in Fig. 7. All amplifications of time amplitude of TI spectrum at frequency of 12 Hz in the output spectrums of TO, T and  $\tau$  are respectively calculated as  $20 \log(TO_{f12}/TI_{f12}) = 20 \log(4\,799/4\,791) \sim 0$  dB,  $20 \log(T_{f12}/TI_{f12}) = 20 \log(14\,382/4\,791) = 9.54$  dB and  $20 \log(\tau_{f12}/TI_{f12}) = 20 \log(9\,598/4\,791) = 6.03$  dB. Very close to this result, show the magnitudes of  $H_T(z)$ ,  $H_T(z)$  and  $H_\tau(z)$  at 12 Hz, in Fig. 5a.

At last, let us find out the amplification and phase delay of the input sinusoidal signal at the output  $\tau$ , using time presentation in Fig. 6. Using proportionality on the magnified Fig. 6, we can find, that since  $A_{TI} = 2 \cdot 8 = 16$  t.u., then  $A_\tau = 32$  t.u. The amplification is  $20 \log(A_\tau/A_{TI}) = 6.02$  dB. This result is very close to the results we have already got from Figs. 5a and 7. Using proportionality on the magnified Fig. 6, we can also find, that the ratio between time delay  $t_d$  of  $\tau$  and the period  $T_{TI}$  is  $|t_d/T_{TI}| = 42/85$ . The phase delay of  $\tau$  is  $360^\circ \cdot (42/85) \sim 178^\circ$ . This result is very close to the phase of frequency response of  $H_\tau(z)$  at 12 Hz, shown in Fig. 5b.

#### 4. CONCLUSIONS

The description and illustrations of the described TNP FLL of the third order represent the additional contributions to the design of TNP FLL of the second order, described in ref. [1]. This work also represents the contribution to the recently described TRP PLL and TRP FLL, which are based on the processing of the input and output periods.

The described TNP FLL is very fast. It takes only 3 steps to reach the stable state, no matter what kind of input is

entered. It reaches the stable state through the step when the algorithm starts using all system parameters. It was shown that this FLL can be very efficiently used for the tracking of a step, a ramp, and an accelerated input function, unlike of TNP FLL of the second order, described in ref. [1], which is not able to track an accelerated input function. This TNP FLL is very scalable to the very wide and strict requirements in the fields of tracking and predicting.

One of contributions of the article is the described methodology procedure for the analyzes of TNP FLL of the third order in the frequency domain as well as the demonstrated closed loop of the time-frequency checks, which confirmed that all time and frequency analyzes are correct. These results and the results in ref. [1], for the TNP FLL of the second order, are a guide which presents how to develop and test TNP FLLs of higher order.

Very important contribution of the article is the presented general form of the difference equation of TNP FLL of any order, intended for the real time applications. It was proved that this general equation of TNP FLL and the difference equation of the digital FIR filters possess very similar structural form, due to which, it was possible to use the theory of digital FIR filters in frequency analyzes and design of TNP FLL. It was proved that TNP FLL represents a kind of digital filter, which is suitable for the filtering of pulse periods. It was shown, for the first time in literature, that TNP FLL described provides even three outputs and that all of them represent digital filters with the different filter properties, even for the same system parameters. Thanks to the ability to use three outputs instead of one and the ability to change widely system parameters, TNP FLL has great options for adapting filter features to the different application requirements.

This article provides a comprehensive basis for the development of a new kind of digital filters, intended for the filtration of the pulse periods.

#### ACKNOWLEDGEMENTS

This article was supported by the Ministry of Science and Technology of the Republic of Serbia within the project TR 32047.

Received on December 22, 2019

#### REFERENCES

- Dj.M. Perisic, V. Petrovic, B. Kovacevic, *Frequency locked loop based on the time nonrecursive processing*, Engineering, Technology & Applied Science Research, **8**, 5, pp. 3450-3455 (2018).
- Dj.M. Perisic, M. Bojovic, *Application of time recursive processing for the development of the time/phase shifter*, Engineering, Technology & Applied Science Research, **7**, 3, pp. 1582-1587 (2017).
- Dj.M. Perisic, A. Zoric, M. Perisic, V. Arsenovic, Lj. Lazic, *Recursive PLL based on the measurement and processing of time*, Electronics and Electrical Engineering, **20**, 5, pp. 33-36 (2014).
- Dj.M. Perisic, A. Zoric, M. Perisic, D. Mitic, *Analysis and Application of FLL based on the processing of the input and output periods*, Automatika, **57**, 1, pp. 230-238 (2016).
- Dj.M. Perisic, M. Bojovic, *Multipurpose time recursive PLL*, Rev. Roum. Sci. Techn. – Électrotechn. et Énerg., **61**, 3, pp. 283-288 (2016).
- Dj.M. Perisic, M. Perisic, S. Rankov, *Phase Shifter based on a recursive Phase Locked Loop of the second order*, Rev. Roum. Sci. Techn. – Électrotechn. et Énerg., **59**, 4, pp. 391-400 (2014).
- Dj.M. Perisic, A. Zoric, Dj. Babic, Dj. Perisic, *Decoding and prediction of energy state in consumption control*, Rev. Roum. Sci. Techn. – Électrotechn. et Énerg., **58**, 3, pp. 263-272 (2013).
- Dj.M. Perisic, A. Zoric, S. Obradovic, P. Spalevic, *Application of frequency locked loop in consumption peak load control*, Electrical Review, **R.88**, 1b, pp. 264-267 (2012).
- Dj.M. Perisic, A. Zoric, S. Obradovic, Dj. Perisic, *FLL as digital period synthesizer based on binary rate multiplier control*, Electrical Review, **R.89**, 1a, pp. 145-148 (2013).
- D. Jovcic, *Phase locked loop system for FACTS*, IEEE Transaction on Power System, **18**, pp. 2185-2192 (2003).
- A.S.N. Mokhtar, B.B.I. Reaz, M. Maruffuzaman, M.A.M. Ali, *Inverse Park transformation using cordic and phase-locked loop*, Rev. Roum. Sci. Techn. – Électrotechn. et Énerg., **57**, 4, pp. 422-431 (2012).
- C.C. Chung, *An all-digital phase-locked loop for high-speed clock generation*, IEEE Journal of Solid-State Circuits, **38**, 2, pp. 347-359 (2003).
- F. Amrane, A. Chaiba, B.E. Babes, S. Mekhilef, *Design and implementation of high-performance field-oriented control for grid-connected doubly fed induction generator via hysteresis rotor current controller*, Rev. Roum. Sci. Techn. – Électrotechn. et Énerg., **61**, 4, pp. 319-324 (2016).
- M. Büyüç, M. İnci, M. Tümay, *Performance comparison of voltage sag/swell detection methods implemented in custom power devices*, Rev. Roum. Sci. Techn. – Électrotechn. et Énerg., **62**, 2, pp. 129-133 (2017).
- L. Joonsuk, B. Kim, *A low noise fast-lock phase-locked loop with adaptive bandwidth control-Solid-State Circuit*, IEEE Journal, **35**, 8, pp. 1137-1145 (2000).
- D. Abramovitch, *Phase-locked loops: a control centric tutorial*, Proc. of American Control Conference-2002, Proceedings, **1**, pp. 1-15 (2002).
- R. Vich, *Z Transform Theory and Application (Mathematics and Applications)*, first ed., Springer, 1987.
- G. Bianchi, *Phase-Locked Loop Synthesizer Simulation*, Mc-Hill, Inc. New York, USA, 2005.
- B.D. Talbot, *Frequency Acquisition Techniques for PLL*, Wiley-IEEE Press, 2012.
- C.B. Fledderman, *Introduction to Electrical and Computer Engineering*, Prentice Hall, 2002.
- M. Gardner, *Phase lock techniques*, Hoboken, Wiley-Interscience, 2005.
- S. Winder, *Analog, and Digital Filter Design*, second edition, Elsevier, 2002.